

Microfabrication of magnetostrictive beams based on NiFe film doped with B and Mo for integrated sensor systems

A. Alfadhel, Y. Gianchandani, and J. Kosel

Citation: *J. Appl. Phys.* **111**, 07E515 (2012); doi: 10.1063/1.3679016

View online: <http://dx.doi.org/10.1063/1.3679016>

View Table of Contents: <http://jap.aip.org/resource/1/JAPIAU/v111/i7>

Published by the [American Institute of Physics](#).

Related Articles

Precessional reversal in orthogonal spin transfer magnetic random access memory devices

Appl. Phys. Lett. **101**, 032403 (2012)

Hot spin-wave resonators and scatterers

J. Appl. Phys. **112**, 013902 (2012)

Magnetic domain wall transfer via graphene mediated electrostatic control

Appl. Phys. Lett. **101**, 013103 (2012)

Perpendicular-magnetic-anisotropy CoFeB racetrack memory

J. Appl. Phys. **111**, 093925 (2012)

High sensitivity low field magnetically gated resistive switching in CoFe₂O₄/La_{0.66}Sr_{0.34}MnO₃ heterostructure

Appl. Phys. Lett. **100**, 172412 (2012)

Additional information on J. Appl. Phys.

Journal Homepage: <http://jap.aip.org/>

Journal Information: http://jap.aip.org/about/about_the_journal

Top downloads: http://jap.aip.org/features/most_downloaded

Information for Authors: <http://jap.aip.org/authors>

ADVERTISEMENT



AIP Advances

Special Topic Section:
PHYSICS OF CANCER

Why cancer? Why physics? [View Articles Now](#)

Microfabrication of magnetostrictive beams based on NiFe film doped with B and Mo for integrated sensor systems

A. Alfadhel,^{1,a)} Y. Gianchandani,² and J. Kosel¹

¹*Division of Physical Sciences and Engineering, King Abdullah University of Science and Technology, Thuwal 23955, Saudi Arabia*

²*Department of Electrical Engineering and Computer Science, University of Michigan, Ann Arbor, Michigan 48109, USA*

(Presented 1 November 2011; received 11 October 2011; accepted 30 November 2011; published online 9 March 2012)

This paper reports the development of integrated micro-sensors consisting of 1- μm -thick magnetostrictive cantilevers or bridges with 500 μm in length and conducting interrogation elements. The thin films are fabricated by sputter deposition of NiFe doped with B and Mo, and the magnetic properties are enhanced by field annealing, resulting in a coercivity of 2.4 Oe. In operation, an alternating current applied to the interrogation elements magnetizes the magnetostrictive structures. The longitudinal resonant frequency is detected as an impedance change of the interrogation elements. The magnetostrictive micro-beams provide high resonant frequencies—2.95 MHz for the cantilever and 5.46 MHz for the bridge—which can be exploited to develop sensors of high sensitivity. © 2012 American Institute of Physics. [doi:10.1063/1.3679016]

I. INTRODUCTION

High-performance resonating sensors have attracted interest for many MEMS applications, especially in the field of biological species detection.¹ For such applications, the surface of the sensor is functionalized to specifically bind to a target analyte. Binding of the target causes a change in the resonant frequency, which, in turn, enables analyte detection and quantification.² Recently, devices that utilize magnetostrictive materials for sensing have been investigated. Compared to other options, such as silicon cantilevers, these vibrate in longitudinal direction instead of transverse direction, leading to higher resonant frequencies. This offers the potential advantage of higher sensitivity.

Previous researches showed that magnetostrictive sensors in the form of beams have a high signal quality factor in air, with reasonable signal damping in higher viscosity fluids.^{2,8} Such sensors have been successfully used for physical, chemical, and biological sensing.^{3–6} The materials typically used for magnetostrictive sensor applications are amorphous magnetostrictive ribbons of about 25 μm thickness fabricated by melt spinning. So far, these sensors have been operated by external coils for actuation and sensing. This approach does not easily allow integration using a standard micro-fabrication process, and their potential for miniaturization is limited. Further miniaturization, though, can be expected to yield an increase in sensitivity, since the resonant frequency scales with the inverse of the sensor size. The main challenges for the development of magnetostrictive sensor systems in the micro-scale regime are the fabrication of soft magnetic thin films with high magnetostriction and obtaining a high signal-to-noise ratio. The latter can only be achieved if the interrogation elements are in close proximity with the magnetostrictive material. In this paper, we report the

fabrication of magnetostrictive fixed-free (cantilever) and fixed-fixed (bridge) beams and their integration with microstructures for interrogation on a common chip. The fabricated magnetostrictive material is similar to the commercially available Metglas 2826MB that is characterized by a very small coercivity, which makes it easy to magnetize, and large magnetomechanical coupling, which provides a large mechanical response upon application of a magnetic field. The developed sensor system enables, for the first time, the detection of the resonant frequency of magnetostrictive micro-beams on an integrated device.

II. METHODS

A. Sensor design

The sensor system consists of a magnetostrictive cantilever or bridge of length 500 μm , width 100 μm , and thickness 1 μm fabricated 2 μm above the interrogation elements, which are 23 conducting lines of $10 \times 0.5 \mu\text{m}^2$ arranged parallel to each other with a pitch of 10 μm (Fig. 1). The magnetostrictive beams are actuated by the magnetic field produced by the current I_{AC} applied to the interrogation elements. With I_{AC} 20 mA, a magnetic field of 0.5 Oe per conducting line is produced 2 μm above the interrogation elements. The beam response depends, besides others, on the actuation frequency and will be highest at the resonant frequency.

The longitudinal resonant frequency for the fixed-fixed beams (Eq. (1))⁷ and fixed-free beams (Eq. (2))⁷ can be evaluated as follows:

$$f = \frac{1}{2L} \sqrt{\frac{E}{\rho(1-\nu)}}, \quad (1)$$

and

$$f = \frac{1}{4L} \sqrt{\frac{E}{\rho(1-\nu)}}, \quad (2)$$

^{a)}Electronic mail: ahmed.fadhel@kaust.edu.sa.

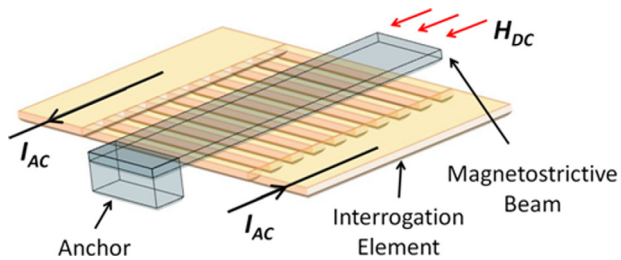


FIG. 1. (Color online) Illustration of the sensor system consisting of a cantilever beam above interdigitation elements. An AC current provides actuation of the cantilever and a DC magnetic field is applied in the longitudinal direction of the beam to set the working point.

where L is the length, E is Young's modulus, ρ is the density, and ν is Poisson's ratio. The Young's modulus for the magnetostrictive material is 100-110 GPa, and the density is 7.54 g/cm^3 . Loading the beam with a mass, for example, a biological target analyte, will change the effective value of ρ . Due to the inverse magnetostrictive effect, the vibration of the beam causes a change of the permeability, which is sensed by the interdigitation elements as a change in impedance. Therefore, the impedance of the interdigitation elements is used to determine the resonant frequency of the beams, which contains the sensing information.

Applying a DC bias field H_{DC} in the longitudinal direction enhances the response of the magnetostrictive beams, which is typically highest around the knee of the magnetization curve. When applying H_{DC} to a magnetostrictive material, the Young's modulus changes⁸ such that

$$E(H_{DC}) = E_0 + \varphi(H_{DC}), \quad (3)$$

where H_{DC} is the applied DC magnetic field, $E(H_{DC})$ is the varying Young's modulus, E_0 is the zero field Young's modulus, and φ is a nonlinear function that relates H_{DC} to the stiffness change. This effect yields a dependence of the resonant frequency on H_{DC} , and it is, therefore, important for H_{DC} to be homogeneous and constant throughout the measurement.

B. Microfabrication process

The developed fabrication process is completed on standard silicon wafers. Patterning of the structures is done through photolithography. First, the interrogating microstructure is patterned. Reactive ion etching is used to etch the Si wafer, and, then the trenches are filled with 500 nm of gold through sputter deposition. The reason for having the interrogating microstructures integrated in the substrate is to reduce the conformal growth for the following layers. A silicon nitride (Si_3N_4) film is deposited to provide electrical isolation between the interrogating elements and the beams. It also serves as an etch stop layer when releasing the beams. In the next step, $2 \mu\text{m}$ of amorphous silicon are deposited with PECVD to be used as the sacrificial layer. In order to create the anchors, the amorphous Si is etched down to the Si_3N_4 film through the use of reactive ion etching. The beams are patterned through bi-layer lift-off lithography to allow easy lift-off with clean edges. The magnetostrictive film fabrication

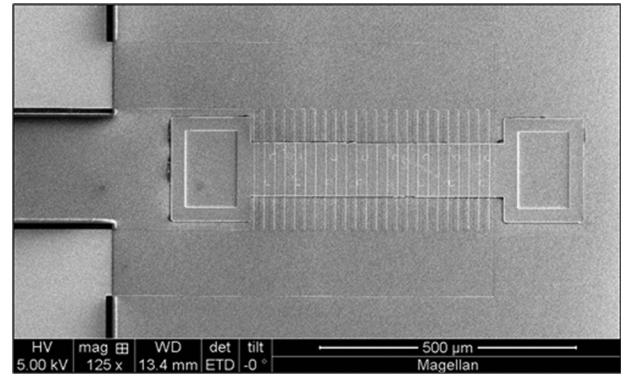


FIG. 2. SEM image of a 500- μm -long bridge with interdigitation structure underneath.

has been optimized in several steps toward low coercivity and is deposited through co-sputtering of $\text{Ni}_{50}\text{Fe}_{50}$, boron (B), and molybdenum (Mo) targets. DC power is used for $\text{Ni}_{50}\text{Fe}_{50}$ (200 W) and Mo (55 W) targets, and RF power is used for B (110 W). To open the gold contact pads of the interdigitation elements, a patterning and etching step through amorphous Si and the Si_3N_4 film is performed using reactive ion etching. Finally, the beams are released by etching the amorphous Si sacrificial film using XeF_2 vapor phase etching. Scanning electron microscopy (SEM), x-ray photoelectron spectroscopy (XPS), and vibrating sample magnetometry (VSM) are used to characterize the properties of the deposited material.

III. EXPERIMENTS AND DISCUSSION

A. Fabrication results

Fig. 2 shows a 500- μm -long bridge fabricated with the developed process. Using XPS, the composition of the deposited magnetic film is found to be $\text{Fe}_{45}\text{Ni}_{31}\text{Mo}_{10}\text{B}_{13}$. Some topography of the interdigitation elements can be observed at the beam surface. The conductive stack deposited into the Si trenches was 90 nm less than the trench depth and, e.g., mechanical polishing would be required before the Si_3N_4 deposition.

B. Magnetic properties

Fig. 3 and Fig. 4 show the magnetization curves in longitudinal and transverse direction, respectively, of a

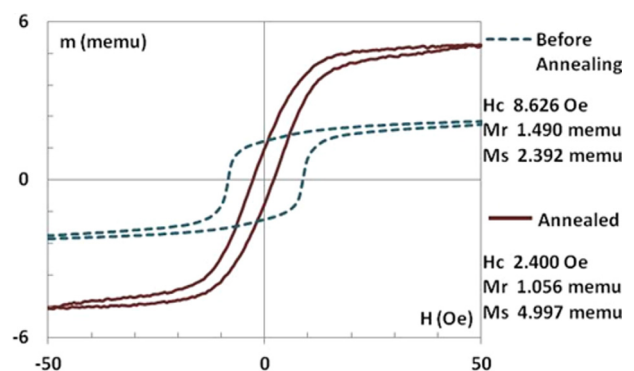


FIG. 3. (Color online) Magnetization curves of a 500- μm -long cantilever in longitudinal direction before and after annealing.

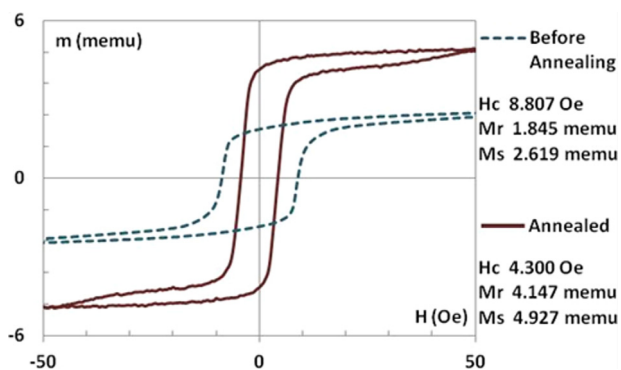


FIG. 4. (Color online) Magnetization curves of a 500- μm -long cantilever in transverse direction before and after annealing.

cantilever before and after field annealing. The as-prepared films are almost isotropic, with a coercivity around 8.6 Oe. After field annealing in the longitudinal direction at 350 °C and 1000 Oe, an induced anisotropy was observed and the coercivity decreased to 2.4 Oe in the longitudinal direction and 4.3 Oe in the transverse direction. The remanence in longitudinal direction became lower after annealing, while the remanence in the transverse direction increased.

C. Resonant frequency measurement

The resonant frequency of the beams is detected by measuring the AC impedance of the interrogation elements. The impedance is measured with an impedance analyzer, applying an AC current I_{AC} of amplitude 20 mA to the interrogation element while sweeping the frequency. An external DC magnetic field H_{DC} of 20 Oe is applied in the longitudinal direction using Helmholtz coils to bias the magnetostrictive sensor to its point of highest sensitivity. The impedances measured for the cantilever and the bridge are shown in Fig. 5 and Fig. 6, respectively. At the resonant frequencies, the impedances exhibit an abrupt change of about 0.1 Ω . The resonant frequencies are found to be 2.95 MHz for the cantilever and 5.46 MHz for the bridge. From Eq. (1) and Eq. (2), the theoretical values of the resonant frequencies are about 4.6 MHz in the case of the bridge and about 2.3 MHz in the case of the cantilever. These values are smaller than the ones

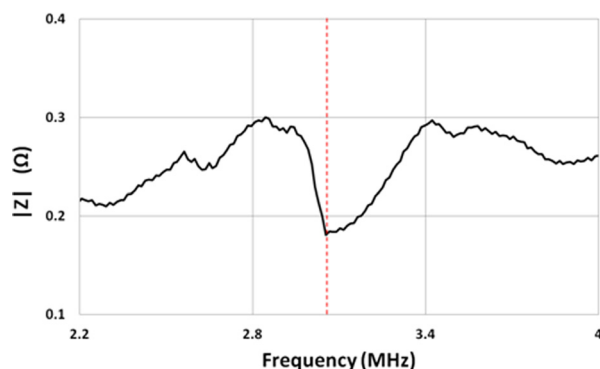


FIG. 5. (Color online) Impedance as a function of the frequency measured for a 500- μm -long cantilever.

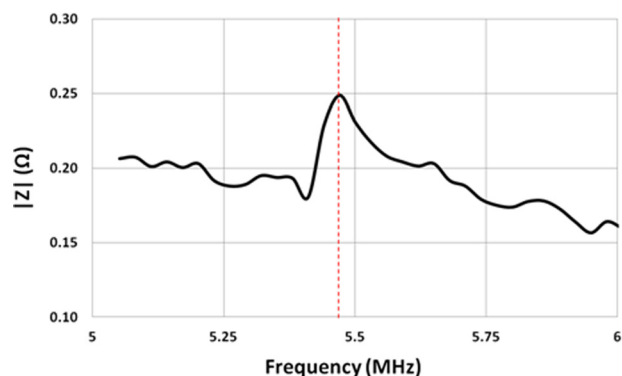


FIG. 6. (Color online) Impedance as a function of the frequency measured for a 500- μm -long bridge.

found experimentally. This is due to the effect of H_{DC} that increases the Young's modulus (see Eq. (3)), which, in turn, yields an increase of the resonant frequency. The resonant frequencies of the cantilever and the bridge are not exactly multiple of each other, which could be due to differences in the effective lengths of the beams. Further studies are conducted to investigate the effect of other vibration modes on the beam longitudinal resonant frequency.

IV. CONCLUSION

A new sensor system using magnetostrictive microbeams and integrated interrogation elements was reported. A thin film process for fabricating soft magnetic, magnetostrictive sensor materials has been developed, including co-sputtering of FeNi, Mo, and B and field annealing to release stress and induce magnetic anisotropy. The integration of 500- μm -long magnetostrictive cantilevers and bridges with conducting interrogation elements is described. The impedance of the interrogation elements clearly showed the resonant frequencies of the magnetostrictive beams, which could be utilized for sensor applications.

ACKNOWLEDGMENTS

This work was supported by the KAUST Global Collaborative Research program. The authors acknowledge the support from the KAUST advanced nanofabrication facility (KANF), especially Ahad Sayed and Dr. Zhihong Wang.

¹M. Ramasamy, C. Liang, and B. C. Prorok, *MEMS and Nanotechnology: Proceedings of the 2010 Annual Conference on Experimental and Applied Mechanics*, Indianapolis, Indiana 2010, edited by Tom Proulx (Springer, New York), Vol. 2, p. 9.

²J. Wan, H. Shu, S. Huang, B. Fiebor, I.-H. Chen, V. Petrenko, and B. A. Chin, *IEEE Sens. J.* **7**, 470 (2007).

³C. A. Grimes, K. G. Ong, K. Loiseau, P. G. Stoyanov, and D. Kouzoudis, *Smart Mater. Struct.* **8**, 639 (1999).

⁴C. Mungle, C. A. Grimes, and W. R. Dreschel, *Sens. Actuators* **101**, 143 (2002).

⁵C. Ruan, K. Zeng, O. K. Varghese, and C. A. Grimes, *Anal. Chem.* **75**, 6494 (2003).

⁶C. Ruan, K. Zeng, O. K. Varghese, and C. A. Grimes, *Biosens. Bioelectron.* **20**, 585 (2004).

⁷C. Liang, *Appl. Phys. Lett.* **90**, 221912 (2007).

⁸S. Green and Y. Gianchandani, *J. Microelectromech. Syst.* **18**, 64 (2009).